



**Michigan
Technological
University**

Michigan Technological University
Digital Commons @ Michigan Tech

Department of Physics Publications

Department of Physics

5-9-2006

Spin-polarized electron transport of a self-assembled organic monolayer on a Ni(111) substrate: An organic spin switch

Haiying Liu

Michigan Technological University

Ravindra Pandey

Michigan Technological University

Ranjit Pati

Michigan Technological University

Shashi P. Karna

US Army Research Laboratory

Follow this and additional works at: <https://digitalcommons.mtu.edu/physics-fp>

 Part of the [Physics Commons](#)


Recommended Citation

Liu, H., Pandey, R., Pati, R., & Karna, S. P. (2006). Spin-polarized electron transport of a self-assembled organic monolayer on a Ni(111) substrate: An organic spin switch. *Physical Review B*, 73.

<http://dx.doi.org/10.1103/PhysRevB.73.195311>

Retrieved from: <https://digitalcommons.mtu.edu/physics-fp/128>

Follow this and additional works at: <https://digitalcommons.mtu.edu/physics-fp>

 Part of the [Physics Commons](#)

Spin-polarized electron transport of a self-assembled organic monolayer on a Ni(111) substrate: An organic spin switch

Haiying He, Ravindra Pandey, and Ranjit Pati*

*Department of Physics and Multi-Scale Technology Institute, Michigan Technological University, Houghton, Michigan 49931, USA*Shashi P. Karna[†]*Weapons and Materials Directorate, U.S. Army Research Laboratory, Aberdeen Proving Ground, Maryland 21005-5069, USA*

(Received 7 November 2005; revised manuscript received 9 January 2006; published 9 May 2006)

Using density functional theory and the Bardeen, Tersoff, and Hamann formalism we have calculated spin-polarized electron transport in a system involving a nonbonded magnetic probe tip and a self-assembled monolayer (SAM) of benzene-1,4-dithiol on a Ni(111) substrate. A significantly higher tunneling current is obtained for a configuration in which the spin of the probe tip is aligned parallel to that of the substrate than for a configuration with antiparallel alignment—an effect prerequisite for an organic spin switch.

DOI: [10.1103/PhysRevB.73.195311](https://doi.org/10.1103/PhysRevB.73.195311)

PACS number(s): 73.40.Gk, 73.61.Ph, 72.80.Le, 72.25.-b

I. INTRODUCTION

The controlled transport of electrons through organic molecule(s) sandwiched between two metal electrodes has been the subject of intense research in recent years because of its potential applications in molecular and molecular-nano hybrid electronics and sensors.^{1–4} Due to the ease of fabricating metal-molecule junctions, one of the frequently used experimental approaches is to tether the molecule to a metal substrate via self-assembly of a molecular monolayer (SAM) and measure the transport properties of such a system using surface probe microscopy, e.g., using scanning tunneling microscope (STM), whose ability to manipulate single atoms and molecules on the substrate has added a new dimension to research in molecular electronics. In fact, STM has been widely used in recent years to study electronic properties of single molecules to self-assembled molecular nanostructures.^{5–7}

In STM measurements involving a SAM, a sample is usually separated from the probing tip by a vacuum gap, and electrons tunnel through the vacuum under an applied bias leading to a finite tunneling current. The tunneling electrons essentially have two degrees of freedom, namely, charge and spin. When tunneling electrons are preferentially aligned (spin up or spin down), the resistance they experience at both the metal-molecule interface and in the molecule is different from the resistance experienced by the unpolarized electrons. The availability of virtually unlimited number of organic molecules, each with unique electronic property offers intriguing possibilities in controlling the spin-polarized current via molecules or monolayer for potential application in molecular spintronics. However, to date, most experiments involving tunneling measurements^{3–7} and theory on molecular devices^{8–14} have focused on the charge state of the electron. Exceptions are a few theoretical calculations on molecular spin valves,^{15–20} and experimental demonstration of spin-dependent transport via a molecular bridge.^{21,22} But all the reported first-principles calculations on molecular spintronics so far deal with strongly coupled metal-molecule junction on both sides of the molecule. Limited attention has been given

to a system involving a SAM on a magnetic substrate probed by a nonbonded magnetic tip. In such an architecture (metal-SAM-vacuum-metal) the sophisticated first-principles-based Keldysh nonequilibrium Green's function formalism¹² in which the tip, the SAM, and the substrate are treated by considering a single cell, may not be suitable because of the inherent difficulty in treating the long-range, nonbonded interaction in the density functional approach. In the present paper, our main objective is to use a SAM of a prototypical benzene-1-4-dithiol (BDT) molecule, which has been studied extensively, on a Ni(111) substrate and probe the spin-polarized tunneling current via the SAM using a nonbonded Ni tip. The specific questions we would like to address are the following. How does the nonbonded configuration at one end of the molecule affect the spin polarized current? Do we observe a similar spin valve effect (parallel spin configuration giving higher current) as observed in strongly coupled metal-molecule systems? Does the magnetoresistance increase or decrease by introducing the SAM on the Ni substrate?

In order to address these subtle questions, we have used density functional theory in conjunction with the Bardeen, Tersoff, and Hamann (BTH) formalism of electron tunneling to calculate the spin-polarized current in a metal-SAM-vacuum-metal architecture. The calculated results show that the tunneling current strongly depends upon the orientation of the electron spins at the probe tip and the substrate. It is important to point out here that the Ni substrate and the monolayer together are considered as a single magnetic domain. To model a realistic description of the tip shape, which is often ignored in theoretical modeling, its cap configuration is varied from a single atom to a cluster involving several atoms to study the shape dependent electron tunneling feature of the tip. We artificially broadened the density of states for various cap configurations using a Gaussian broadening scheme of width 0.2 eV (\sim a few $k_B T$ at room temperature) to take into account the broadening due to the semi-infinite nature of the tip. A parallel alignment of the spins at the tip with respect to the substrate yields significantly higher current than the antiparallel alignment—an effect prerequisite for an organic spin switch.

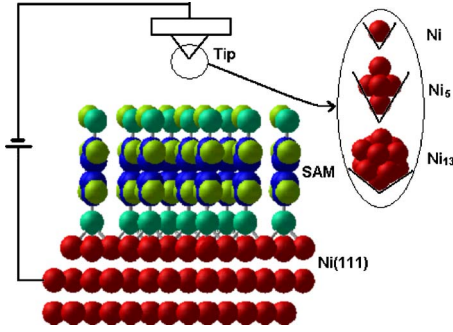


FIG. 1. (Color online) A schematic illustration of the self-assembled BDT monolayer on the Ni(111) substrate and the Ni probe tip in a STM experiment. Notation: red (dark gray), Ni; cyan (light gray), S; blue (black), C; green, (white) H.

The rest of the paper is organized as follows. Section II presents a brief description of the theoretical approach, and Sec. III the results and discussion. In Sec. IV we provide a brief summary of our main results.

II. THEORY

Assuming elastic scattering and neglecting spin-flip scattering and spin precession in the tunneling process because of the weak spin-orbit and hyperfine interaction expected in the π -conjugated organic layer,²¹ the spin-polarized electron tunnel current between two magnetic electrodes can be written as $I = I^\uparrow + I^\downarrow$, where I^\uparrow and I^\downarrow are the contributions from spin-up and spin-down states. In the low-bias limit, $I^{\uparrow(\downarrow)}$ for the system considered in this study can be calculated in the framework of the Bardeen-Tersoff-Hamann and Lang formalism at finite temperature^{23,24} as follows:

$$I^{\uparrow(\downarrow)} = \frac{2\pi e}{\hbar} \gamma \int_{-eV/2}^{eV/2} \rho_s^{\uparrow(\downarrow)} \left(\varepsilon + \frac{eV}{2} \right) \rho_t^{\uparrow(\downarrow)} \left(\varepsilon - \frac{eV}{2} \right) \times e^{-2d\sqrt{2(m/\hbar^2)(\phi_{av}-\varepsilon)}} \left\{ \left[f \left(\varepsilon - \frac{eV}{2} \right) \right] \left[1 - f \left(\varepsilon + \frac{eV}{2} \right) \right] - \left[f \left(\varepsilon + \frac{eV}{2} \right) \right] \left[1 - f \left(\varepsilon - \frac{eV}{2} \right) \right] \right\} d\varepsilon, \quad (1)$$

where $\rho_s^{\uparrow(\downarrow)}$ and $\rho_t^{\uparrow(\downarrow)}$ are the spin-up (-down) projected densities of states (DOSs) of the monolayer and the tip cap, respectively, d is the distance of the tip from the monolayer, ε is the injection energy of the tunneling electron, e is the electronic charge, m is the effective mass of the electron, \hbar is the Planck constant, ϕ_{av} is the average work function of the monolayer and the tip, and f is the Fermi distribution function. As we are interested in the low-bias regime (e.g., $E < 0.5$ eV), the effective mass of the electron (m) and the average work function (ϕ_{av}) are assumed to be constant under applied bias. To match the respective electrochemical potentials at zero bias, the Fermi energy of the monolayer on Ni and the probe tip is aligned and taken to be the reference energy in Eq. (1). γ , a proportionality constant, is assumed to be 1, giving a physical meaning to the calculated tunnel current within the error allowed in the s -wave model approxi-

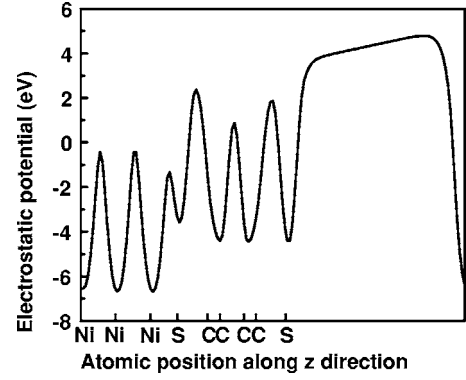


FIG. 2. The planar average electrostatic potential along the z direction for one unit cell of the BDT monolayer coated on Ni(111).

mation of Tersoff and Hamann. It should be pointed out that we have not included the bias-induced changes on the SAM density of states, which is important in the case of high applied bias. In such cases, one needs to include spin-flip effect. In the case of a molecular system, in the presence of low applied bias no significant shift in molecular spectra has been reported,^{9,18} suggesting that one does not expect a significant change in tunneling current in the low-bias regime that we have considered here.

III. RESULTS AND DISCUSSION

A supercell of size $2 \times \sqrt{3}\mathbf{R}$ in the xy plane parallel to the surface and a vacuum of 10 \AA in the z direction for both the Ni(111) substrate and the SAM on Ni are used for electronic structure calculations. A three-layer slab with four Ni atoms per layer is used to simulate the bare Ni substrate, while a BDT molecule adsorbed perpendicularly at the threefold fcc site²⁵ of Ni(111) is used to model the SAM (Fig. 1). Since the adsorption-related relaxation effect in the substrate is expected to be small as we move away from the top layer of the slab, the innermost layer of Ni is kept fixed at the bulk equilibrium geometry. The structural relaxation is carried out with a minimum force criterion of 0.03 eV/\AA on individual atoms. The tip is considered to be separated from the SAM by a rectangular vacuum barrier of width 5 \AA . To model a realistic description of the tip shape, its cap configuration is varied from a single Ni atom to a Ni cluster involving five and 13 atoms, respectively. The density of states for various cap configurations are broadened using Gaussian broadening scheme of width 0.2 eV to take into account the broadening due to semi-infinite nature of the tip. It is noteworthy to point out that it has been reported from scanning tunneling spectroscopy experiment that the life time broadening of the electrons in a cluster on a surface (which may be used to mimic a STM tip) is of the order of or greater than 0.2 eV .²⁶

Self-consistent spin-polarized electronic structure calculations are performed using the plane-wave pseudopotential approach within gradient-corrected density functional theory (DFT) as implemented in the VASP program package.²⁷ The exchange and correlation effects are treated by the Perdew-Wang 1991 exchange and correlation functional form. Initially, a $4 \times 4 \times 1$ Monkhorst-Pack grid was used for k -point

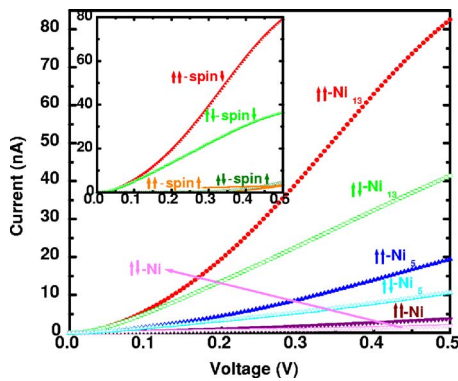


FIG. 3. (Color online) I - V curves for the parallel ($\uparrow\uparrow$) and anti-parallel ($\uparrow\downarrow$) alignments of spins of the tip-molecular wire system. The contribution to the total currents from spin-up (\uparrow) and spin-down (\downarrow) states in both parallel and antiparallel spin alignments is shown in the inset, using Ni_{13} as the tip cap.

sampling of the Brillouin zone which was extended to a $10 \times 10 \times 1$ grid for calculations of densities of states. The cut-off for plane waves is 242 eV, and that for the augmented electron density is 449 eV in these calculations.

A. Structure and magnetic properties

For the adsorbed BDT at the threefold fcc site of Ni(111), the calculated Ni-S bond length is $\sim 2.18 \text{ \AA}$. It is in very good agreement with the length of $2.20 \pm 0.02 \text{ \AA}$ reported for the Ni-S bond in alkane thiolate adsorbed on the Ni(111) substrate.²⁵ For the Ni(111) substrate, a very small ($\sim 1\%$) contraction of the bond distance from its bulk value is obtained, while an outward expansion of about 0.4% in the direction of the adsorbed molecule is predicted for the case of the SAM on Ni. For the Ni(111) substrate, the magnetic moment per atom is $0.69 \mu_B$, which is in agreement with the previously reported value of $0.66 \mu_B$ obtained using the full potential linearized augmented plane wave method.²⁸ In the case of a SAM on Ni, the magnetic moment per Ni atom is $0.62 \mu_B$.

B. Work function

The work function of the SAM, defined as the energy difference between the vacuum-level potential and the Fermi energy level of its surface, is calculated to be $\sim 4.4 \text{ eV}$. The vacuum-level potential is calculated from the planar average of the electrostatic potential in the unit cell (Fig. 2). Since the shape of the cap configuration of the tip is varied, one would expect the potential required to remove the electron from a tip having a different cap to be different. In order to take this shape-dependent feature of the tip into account in this simple model, we have used the corresponding ionization potentials [i.e., 7.62, 6.22, and 5.88 eV for Ni, Ni_5 , and Ni_{13} , respectively (Ref. 29)] and have added the work function of the SAM surface to them to obtain the average work function (ϕ_{av}).

C. Tunneling current

Figure 3 shows the calculated current for the configura-

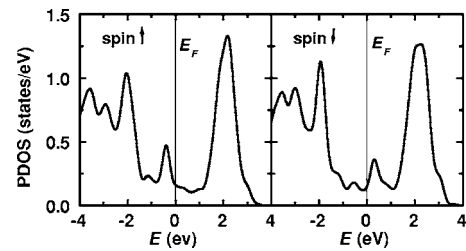


FIG. 4. The projected density of states of the BDT monolayer on Ni(111). Zero of the energy is aligned with the Fermi energy.

tion in which the spin of the tip is aligned parallel (antiparallel) to that of the substrate. The different current for the spin-up and spin-down states (shown in the inset of Fig. 3) can be attributed to the large imbalance between the spin-up and spin-down DOSs of the SAM (Fig. 4) and the tip (Fig. 5) in the immediate vicinity of the Fermi energy. The exchange interaction between the parallel spins of the valence and core states of the Ni atom induces a strong spin polarization in the DOS of the tip and the Ni substrate. After molecular adsorption, the spin-polarized d states of the Ni substrate hybridize with the p states of the S atom of the BDT molecule, polarizing the spin in the monolayer. The spin polarization factor $P = (D_{up} - D_{dn}) / (D_{up} + D_{dn})$, in the monolayer is found to fluctuate from 4% to 45% corresponding to the variation in the injection energy from 0.0 to 0.3 eV. Because of the spin polarization at both the magnetic substrate and the organic monolayer, the spin-up and spin-down carriers experience different scattering potentials leading to different mean free paths, and hence yield a different current. A higher I^\downarrow suggests that the spin-down electrons are the majority carrier in the configuration considered in which the spin-down π^* molecular orbital of the monolayer appears to be the primary channel for the tunnel current. It is important to point out that since *a priori* information about the exact broadening of the energy spectra of the cap due to semi-infinite nature of the tip is not available, we considered a Gaussian broadening of 0.2 eV width for the cap configuration. To study the effect of the larger width on the tunneling and magnetoresistance, we calculated the spin-polarized tunneling current for the five-Ni-atom cap configuration by considering a different smearing width of 0.3 eV. The results are summarized in Fig. 6. The increase in current for both parallel and antipar-

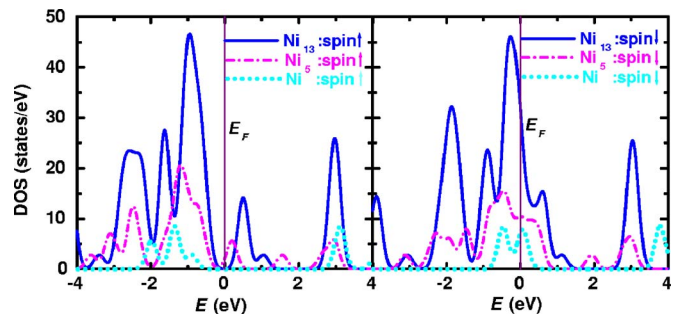


FIG. 5. (Color online) The projected density of states of the probe tip cap consisting of a Ni atom, a Ni_5 cluster, and a Ni_{13} cluster, respectively. The energy levels are broadened using a Gaussian smearing of width 0.2 eV.

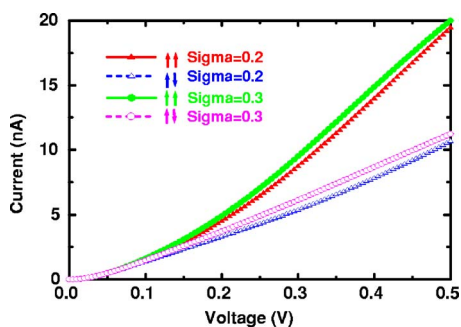


FIG. 6. (Color online) I - V curves for the parallel ($\uparrow\uparrow$) and antiparallel ($\uparrow\downarrow$) alignments of spins of the tip-molecular wire system with Ni_5 as the cap configuration. Sigma represents the width of the Gaussian smearing used to take into account the semi-infinite nature of the tip.

allel spin configuration is evident in the case of stronger broadening as expected. But the increase in current due to larger broadening is found to be the same for both parallel and antiparallel configurations, suggesting that the magnetoresistance value is not affected by broadening.

It is found that the tunneling current in the parallel alignment of spins between the tip and the substrate is significantly higher than the current in the antiparallel alignment. It is important to note that the probe tip and the SAM on a Ni substrate are considered each to be a single magnetic domain. For example, the tunneling current in the parallel alignment is found to be about 99.5% higher in the case of a Ni_{13} cap at 0.5 V. A similar effect has been observed earlier in magnetic single-molecule junctions^{17,18} and has recently been demonstrated experimentally in magnetic organic monolayer junctions.²² The electron tunneling probability from the tip to the SAM can be characterized by a response at the SAM due to a perturbation at the tip under applied bias, which depends primarily upon the convolution of the projected density of states of the tip cap and the SAM at the position of the tip. The larger current in the parallel configuration is due to stronger convolution of the occupied spin-up (-down) DOS of the tip cap with the unoccupied spin-up (-down) DOS of the SAM at the position of the tip. In contrast, the current in the antiparallel configuration is due to convolution of the occupied spin-up (-down) DOS of the tip cap with the unoccupied spin-down (-up) DOS of the SAM at the tip position.

By fitting the linear part of the I - V curve, the resistances associated with parallel (R_P) and antiparallel (R_{AP}) spin alignments are obtained. The calculated values for R_P and R_{AP} are 4.5 M Ω and 10.7 M Ω , respectively, for a Ni_{13} cap, leading to a change in magnetoresistance $(R_P - R_{AP})/R_{AP}$ of about 57%. The calculated changes in magnetoresistance for Ni and Ni_5 cap configurations are 54% and 51%, respectively. As shown in Fig. 3, the absolute magnitude of the tunneling current is found to depend sensitively on the shape of the tip cap. The increase in current for the Ni_{13} cap configuration is solely due to the increase in projected density of states of the Ni_{13} cap near the Fermi energy (Fig. 5) as well as the smaller average work function for the Ni_{13} cap configuration. It is noteworthy to point out here that our empha-

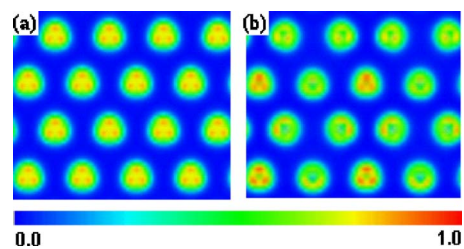


FIG. 7. (Color online) The magnetization density of the Ni surface layer (a) before (left), and (b) after (right) the deposition of the SAM. The color scale goes from blue (black) for very small magnetization density to yellow (white) for larger magnetization density to red (dark gray) for largest magnetization density.

sis is on the relative difference in the tunnel current calculated for the parallel and antiparallel spin configurations, not on the absolute magnitude of the tunnel current, as the calculations assume the proportionality factor γ to be 1 in Eq. (1). The change in magnetoresistance essentially remain the same for the three different cap configurations of the tip.

Note that the calculated tunnel current between the probe tip and the magnetic substrate without the organic monolayer (i.e., ~ 13 Å vacuum barrier) is relatively very small, though the current in the parallel alignment is significantly higher than that in the antiparallel alignment, suggesting higher magnetoresistance ($\sim 90\%$) in the case of the bare Ni-vacuum-Ni tip configuration. It is obviously due to the presence of a larger polarization in the density of states associated with the Ni surface atoms in the absence of the monolayer. A passive barrier is therefore offered by the organic monolayer in the magnetic tip-SAM (substrate) configuration considered in the present study. It is important to point out that though Ni-substrate-vacuum-Ni architecture provides higher magnetoresistance, it will not be of practical use as controlled spin-polarized transport through the vacuum cannot be feasible. On the other hand, different molecules will endure different degrees of spin polarization due to their interaction with the magnetic substrate, thus offering a viable medium for controlled spin-polarized transport, a main theme in molecular spintronics.

D. Magnetization density

The magnetization density calculated on the Ni(111) surface (a) in the absence and (b) in the presence of a molecular SAM is shown in Fig. 7. The bare Ni(111) surface clearly shows a uniform magnetization. In contrast, the surface with the SAM has nonuniformity in the magnetization density. Furthermore, the three Ni atoms that are bonded to the S atom of the molecule have lower magnetization density compared to the nonbonded Ni atom. This is due to the electron transfer from the monolayer to the d down-spin band of the bonded Ni atoms on the substrate arising from the hybridization between the Ni d orbital and the p orbital of S, suggesting a dominant bond-mediated electron tunneling mechanism at the interface.

IV. CONCLUSIONS

In summary, we have investigated the spin-polarized electron tunneling mediated by an organic molecule between two

magnetic electrodes (one being the nonbonded electrode) using periodic DFT in conjunction with the BTH electron tunneling formalism. The calculations show that the absolute magnitude of the tunnel current depends sensitively upon the shape of the tip cap, suggesting that a spatially broadened wave function at the tip is more effective in electron transport than a constrained wave function. However, the change in magnetoresistance is found to be essentially the same for the three different cap configurations of the tip. The calculated results also show that the spin-polarized electron tunneling strongly depends on the relative orientation of the spin at the substrate and the probe tip. A parallel alignment of the spin at the probe tip with respect to that at the substrate results in a higher magnitude of the tunnel current than the antiparallel alignment—an effect prerequisite for an organic spin switch. It is expected that the present calculation will have a direct relevance to the widely used STM experiment in which a nonbonded tip is usually used to measure the tunneling current across molecular wires. We suggest that by considering a magnetic tip and magnetic substrate, one will

be able to observe this switching effect. Since the magnetic tip dimension is much smaller than the dimension of the substrate, the coercive field for it will be different from that of the substrate. Thus one can easily change the spin configuration at the tip with respect to the substrate using an external magnetic field.

ACKNOWLEDGMENTS

We thank Dilip Kanhere, Mrinalini Deshpande, and Andrew Pineda for helpful discussions during this work. This work at Michigan Tech was supported by the Defense Advanced Research Project Agency (DARPA) through Army Research Laboratory (ARL) Contract No. DAAD17-03-C-0115 and by the National Computational Science Alliance through Grant No. ASC050006N. One of the authors (H.H.) also acknowledges support from the Dow Corning Foundation. The work at Army Research Laboratory was partially supported by the Director Research Initiative (Grant No. FY05 WMR-01).

*Corresponding author. Electronic address: patir@mtu.edu

†Corresponding author. Electronic address: skarna@arl.army.mil

¹A. Nitzan and M. A. Ratner, *Science* **300**, 1384 (2003).

²J. R. Heath and M. A. Ratner, *Phys. Today* **56** (5), 43 (2003).

³M. A. Reed, C. Zhou, D. J. Muller, T. P. Burgin, and J. M. Tour, *Science* **278**, 252 (1997).

⁴C. P. Collier, E. W. Wong, M. Belohradsky, F. M. Raymo, J. F. Stoddart, P. J. Kuekes, R. S. Williams, and J. R. Heath, *Science* **285**, 391 (1999).

⁵R. P. Andres, T. Bein, M. Dorogi, S. Feng, J. I. Henderson, C. P. Kubiak, W. Mahoney, R. G. Osifchin, and R. Reifenberger, *Science* **272**, 1323 (1996).

⁶S. W. Wu, G. V. Nazin, X. Chen, X. H. Qiu, and W. Ho, *Phys. Rev. Lett.* **93**, 236802 (2004).

⁷F. Moresco, G. Meyer, K. H. Rieder, H. Tang, A. Gourdon, and C. Joachim, *Phys. Rev. Lett.* **86**, 672 (2001).

⁸V. Mujica, M. Kemp, A. Roitberg, and M. A. Ratner, *J. Chem. Phys.* **104**, 7296 (1996).

⁹J. Heurich, J. C. Cuevas, W. Wenzel, and G. Schön, *Phys. Rev. Lett.* **88**, 256803 (2002).

¹⁰M. Di Ventra, S. T. Pantelides, and N. D. Lang, *Phys. Rev. Lett.* **84**, 979 (2000).

¹¹A. W. Ghosh, F. Zahid, S. Datta, and R. Birge, *Chem. Phys.* **281**, 225 (2002).

¹²J. Taylor, H. Guo, and J. Wang, *Phys. Rev. B* **63**, 245407 (2001).

¹³S. Datta, W. Tian, S. Hong, R. Reifenberger, J. I. Henderson, and C. P. Kubiak, *Phys. Rev. Lett.* **79**, 2530 (1997).

¹⁴R. Pati and S. P. Karna, *Phys. Rev. B* **69**, 155419 (2004).

¹⁵E. G. Emberly and G. Kirczenow, *Chem. Phys.* **281**, 311 (2002).

¹⁶M. Zwolak and M. Di Ventra, *Appl. Phys. Lett.* **81**, 925 (2002).

¹⁷R. Pati, M. Mailman, L. Senapati, P. M. Ajayan, S. D. Mahanti, and S. K. Nayak, *Phys. Rev. B* **68**, 014412 (2003).

¹⁸R. Pati, L. Senapati, P. M. Ajayan, and S. K. Nayak, *Phys. Rev. B* **68**, 100407(R) (2003).

¹⁹A. R. Rocha, V. M. García-Suárez, S. W. Bailey, C. J. Lambert, J. Ferrer, and S. Sanvito, *Nat. Mater.* **4**, 335 (2005).

²⁰L. Senapati, R. Pati, M. Mailman, and S. K. Nayak, *Phys. Rev. B* **72**, 064416 (2005).

²¹Z. H. Xiong, D. Wu, Z. V. Vardeny, and J. Shi, *Nature (London)* **427**, 821 (2004).

²²J. R. Petta, S. K. Slater, and D. C. Ralph, *Phys. Rev. Lett.* **93**, 136601 (2004).

²³J. Tersoff and D. R. Hamann, *Phys. Rev. Lett.* **50**, 1998 (1983).

²⁴N. D. Lang, *Phys. Rev. B* **34**, 5947 (1986).

²⁵D. R. Mullins, D. R. Huntley, T. Tang, D. K. Saldin, and W. T. Tysoe, *Surf. Sci.* **380**, 468 (1997).

²⁶L. Bolotov, N. Uchida, and T. Kanayama, *Eur. Phys. J. D* **16**, 271 (2001).

²⁷Vienna *ab initio* Simulation Package (Technische Universität Wien, 1999); G. Kresse and J. Furthmüller, *Phys. Rev. B* **54**, 11169 (1996).

²⁸G. B. Grad, P. Blaha, K. Schwarz, W. Auwärter, and T. Greber, *Phys. Rev. B* **68**, 085404 (2003).

²⁹M. B. Knickelbein, S. Yang, and S. J. Riley, *J. Chem. Phys.* **93**, 94 (1990).